Particle Acceleration at Reflected Shocks in Supernovae Remnants

Supervised by Dr Iurii Sushch

Kobus Le Roux

kobusler@gmail.com

Abstract

Supernovae remnants (SNRs) are widely believed to be one of the prime sources of Galactic cosmic rays. They are known to be efficient particle accelerators which is indirectly confirmed by detection of non-thermal emission across the whole electromagnetic spectrum from radio to very-high-energy gamma-rays [1]. Protons and electrons can be accelerated to very high energies of at least several tens of TeV both at the forward and at the reverse shock of the remnant. About 80% of all SNRs originate in core-collapse events and are expected to expand into a complex environment of the stellar wind bubble blown up by their progenitor stars, where forward shock (FS) might interact with various density inhomogeneities. Such interaction would cause the formation of reflected shocks propagating inside the remnant which can potentially be strong enough to also accelerate particles. Current investigations of particle acceleration in SNRs are usually limited to forward and reverse shocks ignoring the complexity of the hydrodynamic picture. Although for most SNRs the observed shell-like morphology generally agrees with an idea that high energy particles originate predominantly from the forward shock (for some remnants the significant contribution from the reverse shock was also confirmed [2]), precise spatially resolved measurements do not always agree with a simplified picture giving rise to alternative ideas such as interaction with dense cloudlets [3]. This work is focused on the investigation of particle acceleration at the reflected shocks formed through the interaction of the forward shock with density inhomogeneities and its potential impact on the overall observational properties.

1 Simulation Tools

For our simulations, we make use of the **R**adiation **A**cceleration **T**ransport **P**arallel **C**ode (RATPaC), developed by the Theoretical Astroparticle group at DESY to numerically solve the partial differential transport equations used to describe the diffusive shock acceleration process in SNRs [4]. These equations are solved in simultaneous conjunction with the PLUTO program, which handles the magnetohydrodynamic evolution of the SNR, and feeding those outputs to RATPaC in real time on the fly.

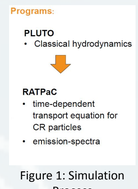

Figure 1: Simulation Process

$$\frac{\partial}{\partial t}\begin{pmatrix}\rho\\ \mathbf{m}\\ E\end{pmatrix}+\nabla\begin{pmatrix}\rho\mathbf{v}\\ \mathbf{m}\mathbf{v}+P\mathbf{I}\\ (E+P)\mathbf{v}\end{pmatrix}^{T}=\begin{pmatrix}0\\0\\0\end{pmatrix}$$

$$\frac{\rho\mathbf{v}^2}{2}+\frac{P}{\gamma-1}=E,$$

Figure 2: Hydrodynamical equations solved

Figure 2 shows the the standard gas-dynamical equations solved by pluto to obtain the evolution of the SNR in a predefined medium. This evolution is treated in a time and spatially dependant way. These equations are solved in 1 dimension and assuming spherical symmetry. Different prescriptions for ejecta profiles are used depending on the type of explosion. For hydro profiles of the ambient medium, we either use some analytic prescriptions or pre-simulated profiles from hydrodynamic simulations of stellar winds

Figure 3 shows the transport equation solved by RATPaC after obtaining the necessary hydrodynamic data from PLUTO. This equation is likewise solved in 1 dimension and assuming spherical symmetry, and also includes synchrotron cooling for electrons. This equation is implemented on a co-moving expanding grid, meaning that there is no free escape boundary, and all particles are contained within the bounds of the simulation.

$$\frac{\partial N}{\partial t}=\nabla\left(D_r\nabla N-\upsilon N\right)-\frac{\partial}{\partial p}\left(N\dot{p}-\frac{\nabla\upsilon}{3}Np\right)+Q$$

Diffusion · Advection · Cooling · Acceleration · Injection

Figure 3:Transport equation solved by RATPaC for cosmic rays

$$x-1=\frac{r}{R_{sh}}-1=(x_*-1)^3$$

Figure 4: Transformation for increased resolution

Figure 4 shows the change of variables used in solving the transport equation to transform the grid from linear binning to a situation where smaller bins are more concentrated around the shock. This increases the resolution around the shock where particle acceleration is expected to occur, in order to obtain more accurate simulation data.

The injection of particles then happens at every timestep, and they are injected with injection momentum $p_{inj} = \xi p_{thermal}$ which is the tail end of the maxwellian distribution.

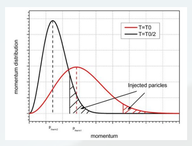

Figure 5: Injection momentum

2 Reflected shock profile

The figure below shows the formation and time evolution of a reflected shock formed when the forward shock (FS) of a SNR interacts with a jump in density. This reflected shock propagates inside the remnant until it interacts with the reverse shock (RS). In this interaction, the reflected shock transfers energy to the RS, accelerating it, and is reflected yet again toward the FS of the SNR, where the same interaction occurs at the contact discontinuity. In this way, the reflected shock can be bounced between the contact discontinuity and RS, oscillating in that region until all energy contained is transferred to both the FS and RS.

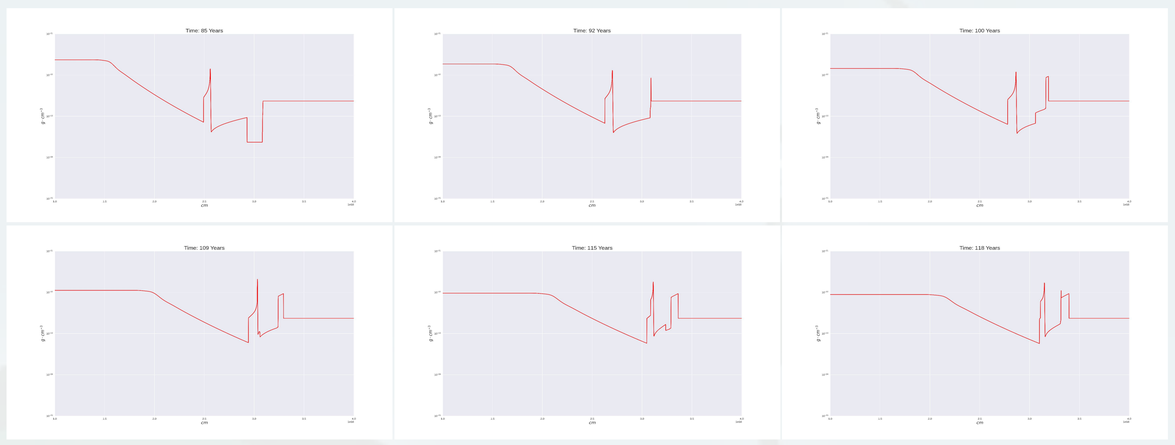

Figure 6: Formation and evolution of reflected shock

3 An interesting pileup of particles

Figure 7 shows the relation between the hydrodynamic profile and the cosmic ray profile for a simulation of a SNR with a Wolf-Rayet as progenitor star. The first panel showcases the timestep where the FS interacts with a jump in density, forming the reflected shock seen in the 2nd panel which propagates backwards through the remnant towards the RS. Comparing the hydrodynamic profile with that of the cosmic ray profile, we see a buildup of energetic particles corresponding to the location of the reflected shock. The question to be answered then becomes if this bump in the cosmic ray profile is due to acceleration of particles by the reflected shock, or is this property seen in the simulation due to some other effect?

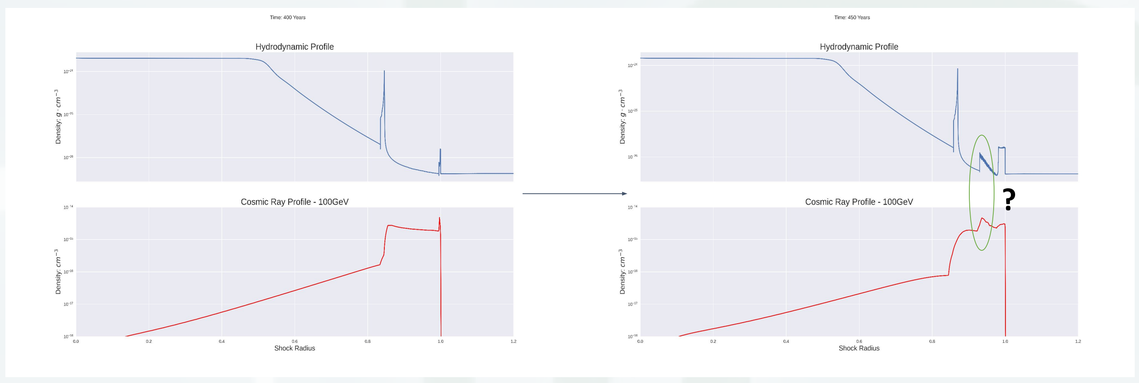

Figure 7: Relation between Hydro and Cosmic Ray profiles

4 Acceleration? An Investigation:

In order to investigate if this pile up of energetic particles observed in the simulation is the result of particles being accelerated by the reflected shock, we directed our vision to the region between the FS and RS through which the reflected shock will propagate (this is the orange region marked with the green circle in figure 8).

Testing particle acceleration in this region involved running the previous simulation depicted in figure 7 again for a second time, but modifying our program to force the acceleration term to be 0 in the region through which the reflected shock propagates. Figure 8 shows a visual representation of this process. By doing this, we ensure that no particles are accelerated in this region for the second simulation, ensuring no contribution from the reflected shock.

After this new dataset is produced, the results from both simulations can be compared to each other. Since one simulation allowed for particle acceleration in the region where the reflected shock propagates and the other didn't, the difference in spectrums produced by both simulations can be used to give an indication of the particle acceleration occurring due to the reflected shock.

$$\frac{\partial N}{\partial t}=\nabla\left(D_r\nabla N-\upsilon N\right)-\frac{\partial}{\partial p}\left(N\dot{p}-\frac{\nabla\upsilon}{3}Np\right)+Q$$

Diffusion · Advection · Cooling · Acceleration · Injection

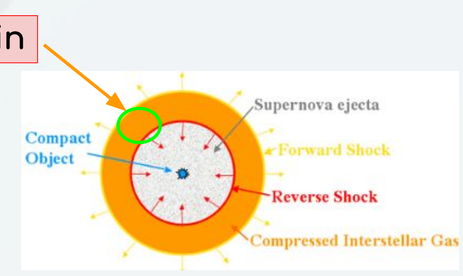

Figure 8: Demonstration of method

5 A weak shock

Figure 9 illustrates the spectra obtained for both simulations. The dashed green line shows the electron energy distribution in the region where the reflected shock propagates for the simulation where the acceleration in this region was disabled. We see that it virtually identical to and doesn't deviate from the red line, which shows the electron energy distribution in the same region for the simulation without the constraints on acceleration. This indicates that there is no significant contribution in acceleration from the reflected shock in this region.

The reason for this is evident when considering figure 10, which shows the temperature and density profiles for the simulation at an arbitrary timestep. Here, we see that in the region between the FS and the RS which the reflected shock propagates through, the temperature is extremely high. A high temperature implies that the speed of sound in the medium is very high, which in turn decreases the mach number of the shock. This means that this reflected shock is a weak shock, unable to efficiently accelerate particles in the medium. It does contribute to the morphology of the SNR, by compressing the particles in the medium, but does not directly contribute to the acceleration of particles, and by extension, the spectra obtained.

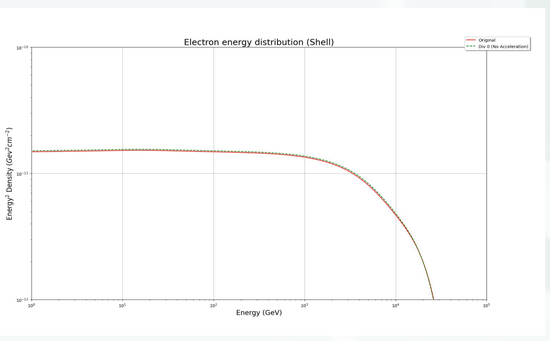

Figure 9: Difference in spectra

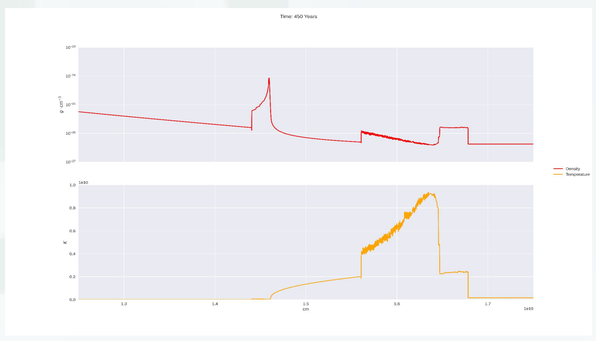

Figure 10: Temperature profile

6 Further consideration: A secondary effect

Observing figure 10, we see that the temperature at the RS is considerably lower than that of the reflected shock. This means that we expect the RS to be accelerating particles efficiently. Remembering form figure 6 that the reflected shock interacts with the RS to accelerate it, it is expected that this interaction will boost particle acceleration across the RS.

A toy model with a 10x jump in density (depicted in figure 11) was created to probe the effect of this interaction on the acceleration of the RS. Figure 12 shows the energy distribution of protons at 3 different timesteps. The blue line at 70 years indicates the timestep just before the interaction between the FS and the density jump, prior to the formation of the reflected shock. The orange line at 120 years gives the timestep after the reflected shock interacted with the RS, accelerating it. The green line at 140 years is included to show the evolution of the energy distribution at a time after the reflected shock interacted with the RS. From figure 12, we see that the FS accelerates particles to lower energies as time continues, as it loses energy from moving through the dense medium.

Figure 13 shows the opposite effect for the RS. Here, we see that the RS becomes a more efficient accelerator of charged particles as time continues, since the energy transferred by the reflected shock accelerates the RS, increasing the Mach number and the strength of the shock.

This indicates that the RS becomes a better accelerator of particles as the SNR evolves, eventually even surpassing the accelerating abilities of the FS as the SNR age. The reflected shock continually interacts with the RS, accelerating it and boosting acceleration even further.

Figure 11 : Toy model Profile

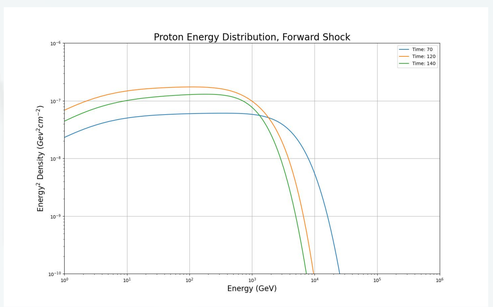

Figure 12: FS evolution of spectra produced

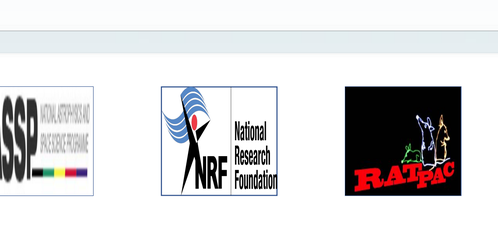

Figure 13: RS evolution of spectra produced

7 Conclusions

- A reflected shock is formed when the FS of a SNR interacts with a sudden jump in density in the medium
- This reflected shock compresses the energetic particles in the region through which it propagates, influencing the morphology of the SNR
- Since the region through which the reflected shock propagates is extremely hot, the speed of sound in this medium is very fast, weakening the shock so that no particles are able to be efficiently accelerated across this shock
- The reflected shock interacts with the RS, accelerating it and boosting particle acceleration across this shock. This property becomes increasingly important in older SNRs, where acceleration at the RS may surpass acceleration at the FS

[1] Reynolds, S., P., Supernova remnants at high energy, Annual Rev. Astron. Astrophys., Vol. 46, p. 89-126 (2008)

[2] Brose, R., et al., Nonthermal emission from the reverse shock of the youngest Galactic supernova remnant G1.9+0.3, Astronomy & Astrophysics, Volume 627, id.A166, 9 pp. (2019)

[3] Sushch, I., and Hnatyk, B., Modelling of the radio emission from the Vela supernova remnant, Astronomy & Astrophysics, Volume 561, id.A139, 8 pp. (2014)

[4] Sushch, I., Brose, R., and Pohl, M., Modeling of the spatially resolved nonthermal emission from the Vela Jr. supernova remnant, Astronomy & Astrophysics, Volume 618, id.A155, 11 pp. (2018)

Tenth International Fermi Symposium, Johannesburg 9th–15th October 2022